Hybrid Bilayer Membranes in Air and Water: Infrared Spectroscopy and Neutron Reflectivity Studies

Curtis W. Meuse,* Susan Krueger,# Charles F. Majkrzak,# Joseph A. Dura,# Joseph Fu,§ Jason T. Connor,* and Anne L. Plant*

*Biotechnology Division, #NIST Center for Neutron Research, and §Precision Engineering Division, National Institute of Standards and Technology, Gaithersburg, Maryland 20899 USA

ABSTRACT In this report we describe the fabrication and characterization of a phospholipid/alkanethiol hybrid bilayer membrane in air. The bilayer is formed by the interaction of phospholipid with the hydrophobic surface of a self-assembled alkanethiol monolayer on gold. We have characterized the resulting hybrid bilayer membrane in air using atomic force microscopy, spectroscopic ellipsometry, and reflection-absorption infrared spectroscopy. These analyses indicate that the phospholipid added is one monolayer thick, is continuous, and exhibits molecular order which is similar to that observed for phospholipid/phospholipid model membranes. The hybrid bilayer prepared in air has also been re-introduced to water and characterized using neutron reflectivity and impedance spectroscopy. Impedance data indicate that when moved from air to water, hybrid bilayers exhibit a dielectric constant and thickness that is essentially equivalent to hybrid bilayers prepared in situ by adding phospholipid vesicles to alkanethiol monolayers in water. Neutron scattering from these samples was collected out to a wave vector transfer of 0.25 $Å^{-1}$, and provided a sensitivity to changes in total layer thickness on the order of 1–2 Å. The data confirm that the acyl chain region of the phospholipid layer is consistent with that observed for phospholipid-phospholipid bilayers, but suggest greater hydration of the phospholipid headgroups of HBMs than has been reported in studies of lipid multilayers.

INTRODUCTION

Many methods for preparing supported lipid bilayers have been described (Tamm and McConnell, 1985; Tien, 1990; Lang et al., 1992; Florin and Gaub, 1993; Stelzle et al., 1993; Erdelen et al., 1994; Plant et al., 1994; Duschl et al., 1996). Planar supported mimics of cell membranes are of interest for membrane structure/function studies (Meuse et al., 1998; Kalb et al., 1992), and for applications such as pharmaceutical screening, biosensors, and bioelectronics (Tien, 1990; Stelzle et al., 1993; Plant et al., 1995; Gizeli et al., 1996). Structural analysis of supported bilayer membranes would be enhanced by the ability to apply certain techniques that are more difficult in, or not compatible with, aqueous conditions, such as x-ray photoelectron microscopy, scanning tunneling microscopy, reflection-absorption infrared spectroscopy, and ellipsometry. Lipid membrane mimics are more likely to be attractive for commercial applications if they could be stored in air or in an inert atmosphere. The ability to dehydrate a single lipid bilayer would also allow new ways of studying how water influences the structure of lipid membranes and their proteins.

Here we report a method for the transfer of a single layer of phospholipid from the air-water interface onto a hydrophobic alkanethiol-coated gold surface (see Fig. 1) to form an air-stable hybrid bilayer membrane (HBM). The technique we describe differs from that described by Tamm and McConnell (1985) in which a monolayer of lipid from the air-water interface was added to a monolayer-coated substrate by immersing the substrate horizontally through the interface. In that technique, the bilayer was kept continuously under water. In the method we report here, we lower a hydrophobic substrate horizontally into the air-water interface and lift it out into air, carrying lipid from the interface with it. Atomic force microscopy, reflection-absorption infrared spectroscopy, and ellipsometry have been used to characterize these hybrid bilayers in air. The continuity and order of the phospholipid layer is demonstrated, and these HBMs are compared to HBMs formed in situ from alkanethiol monolayers and phospholipid vesicles.

These layers can also be rehydrated as demonstrated by impedance spectroscopy and neutron reflectivity measurements. Neutron reflectivity (Majkrzak and Felcher, 1990) is well-suited to the study of structure and structural changes in lamellar systems such as lipid monolayers, bilayers, multilayers, and biological membranes. Several recent experiments have focused on the study of streptavidin binding to biotinylated lipid monolayers either at the air-water interface (Vaknin et al., 1991; Loesche et al., 1993), or adsorbed onto solid substrates (Schmidt et al., 1992). More complicated mixed monolayers of lipid and surfactant at the air-water interface have also been studied with neutrons (Naumann et al., 1994). The structure of dimyristoyl phosphatidylcholine (DMPC) bilayers adsorbed onto planar substrates has been studied by Johnson et al. (1991). Reinl et al. (1992) used neutron reflectivity to measure changes in the thickness of single dipalmitoyl phosphatidylcholine (DPPC)

Received for publication 24 July 1997 and in final form 21 November 1997.

Address reprint requests to Dr. Anne L. Plant, Chemistry A353, NIST, Gaithersburg, MD 20899. Tel.: 301-975-3124; Fax: 301-330-3447; E-mail: tree@micf.nist.gov.

Jason T. Conner's present address is Biomedical Engineering Department, Case Western Reserve University, Cleveland, OH.

0006-3495/98/03/1388/11 $2.00

bilayers on quartz surfaces after the incorporation of cholesterol. Measurements on single phospholipid/phospholipid bilayers on silicon (Krueger et al., 1995; Koenig et al., 1996), under similar experimental conditions to those described here, have been reported.

In this report, a combination of a small cell volume and the absence of vesicles in solution reduces the incoherent background scattering of neutrons. As a result, we are able to measure neutron scattering out to a wavevector transfer of 0.25 $Å^{-1}$, and achieve a sensitivity of 1–2 Å in overall bilayer thickness. Differences in the thickness of the phospholipid layer above and below the phase transition temperature were clearly observed.

METHODS

The gold surfaces for reflection-absorption infrared spectroscopy (RAIRS), impedance spectroscopy, and spectroscopic ellipsometry were prepared by thermal evaporation of ~100 Å chromium, then ~2000 Å gold (99.9%) at a base pressure of $\sim 1 \times 10^{-3}$ Pa onto silicon(111) wafers (Virginia Semiconductor, Fredericksburg, VA) at room temperature. [The specification of commercial products is for clarity only, and does not constitute endorsement by the NIST.] The gold surfaces for AFM (130 Å thick) and neutron reflectivity (50 Å thick) were prepared using a Millatron DBS Model 3424 thermal evaporation and ion milling system (Commonwealth Scientific, Alexandria, VA) (Pedulla and Deslattes, 1993), and were deposited on 15-Å barrier films of chromium or titanium. For atomic force microscopy (AFM), the substrates were 1″ × 1″ × ¼″ silcon(111). For neutron reflectivity, the substrates were 4″ diameter by 3/16″ thick silcon(111). A Digital Instruments stand-alone contact AFM with a Si_3N_4 pyramid type tip was used to characterize the Millatron gold surfaces. A Fabry-Perot interferometer was used to monitor the displacement of the cantilever, providing force information for a given force constant. During operation, a known force is maintained between the surface and the tip by using a feedback circuit to expand or contract the Z-piezoelectric element to keep a constant separation between the cantilever and the light source. The AFM revealed the root mean squared (RMS) roughness of gold surfaces prepared by the Millatron to be ~0.16 nm for an area of 1 μm × 1 μm (see Fig. 2).

Alkanethiol monolayers were prepared by immersing the gold-coated substrates in 1 mmol/l octadecanethiol (Aldrich, Milwaukee, WI, 97%) solutions in 200 proof ethanol (Warner Graham Co., Cockeysville, MD) for a minimum of 12 h. The phospholipids used in these studies were DMPC, DPPC, disteroyl phosphatidylcholine (DSPC), and the deuterated acyl chain analog of DPPC (DPPC-d_{62}); all were purchased from Avanti Polar Lipids (Alabaster, AL). Lipid bilayer vesicles of DMPC or DPPC were formed by the injection method (Batzri and Korn, 1973). An isopropanol solution (50 μl) of lipid was injected with a syringe, while vortexing, into 1 ml 20 mmol/l Tris, 150 mmol/l NaCl, pH 7.0 (TBS) held above the gel to liquid crystalline phase transition temperature of the lipid. The final lipid concentration was 2 mmol/l.

To illustrate the method used for producing HBMs in air, a diagram of the stages involved in horizontal transfer of phospholipid is shown in Fig. 1. Lipid is spread at the air-water interface of a Nima 2011 Langmuir-Blodgett trough (Coventry, England). The barriers are controlled to maintain a surface pressure of 48mN/m during transfer. The alkanethiol-coated gold substrate is positioned parallel to the surface and lowered until it makes contact with the air-water interface and the interfacial lipid. When the substrate is raised, the surface tension of the water prevents the immediate separation of the sample surface and the water. Fig. 1 illustrates that the air-water interface curves back under the wafer, carrying two lipid layers sandwiching a layer of water. The difference in the area occupied by lipid at the interface indicates a transfer ratio of 200 ± 4%. If the water is allowed to dry either under ambient conditions or in a stream of nitrogen,

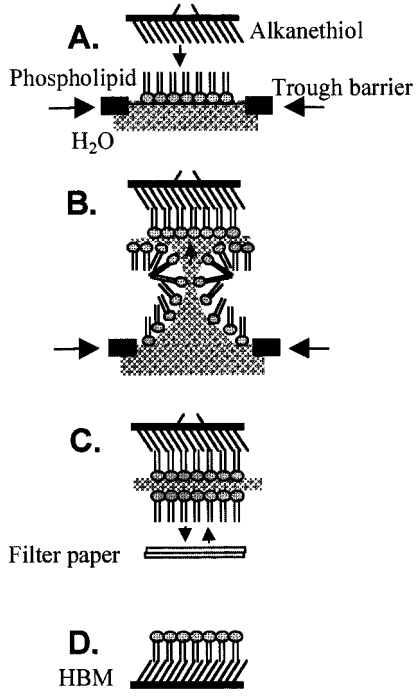

FIGURE 1 Illustration of the method of formation of an HBM in air by transfer of phospholipid from the air-water interface, and the removal of the water layer and associated excess lipid.

approximately two layers of phospholipid are associated with the alkanethiol monolayer, effectively forming a trilayer.

In order to remove the second outer layer of lipid, the wet sample is simply blotted gently on a stack of several sheets of filter paper (Whatman #1) as shown in Fig. 1. As the layer of water is removed from the surface, it carries the extra lipid layer with it.

Hybrid bilayers formed by this method were compared with HBMs formed from the reorganization of lipid vesicles in situ at hydrophobic alkanethiol monolayer surfaces. To prepare HBMs in situ, a solution of lipid vesicles was placed onto a thiol-coated substrate for 90 min to allow formation of the bilayer. For impedance analysis, this incubation period occurred in the electrochemistry cell. To rinse vesicles from the surface, the vesicle solution was partially removed and water was added to dilute the solution in such a manner that the surface was never dry. For impedance analysis, the cell was then filled with electrolyte solution. For other measurements, after at least eight rinsing cycles, the excess water was removed by blotting the surface with a stack of several sheets of filter paper.

Ellipsometry measurements were obtained using an M-44 spectroscopic ellipsometer from J. A. Woollam Co. (Lincoln, NE). Analysis of the data was performed using the accompanying software. A two-layer model was adopted to analyze the surfaces, where the alkanethiol-coated gold surface comprised layer one, and the phospholipid constituted layer two. A single set of optical constants for layer one was determined by acquiring an ellipsometric spectrum over the range of 419 to 761 nm in the absence of the phospholipid layer and fitting the data by nonlinear least squares analysis to the best optical constants. Phospholipid layer thicknesses were obtained by repeating the analysis on the sample with the phospholipid layer, using a refractive index for the phospholipid layer of 1.45 (Lang et al., 1992) and the optical constants determined for layer one.

The RAIRS spectra were obtained at room temperature on a Mattson Research Series 2 spectrometer (Madison, WI) with a Harrick (Ossining, NY) 75° reflection accessory with a built-in polarizer. Each spectrum was the result of integrating 1000 scans; 10 sample spectra and corresponding background spectra from the same gold substrate were collected, ratioed to one another, and the results were averaged to produce representative

spectra at 4 cm^{-1} resolution. Spectral analysis was performed using Grams 386 software (Galactic Industries, Salem, NH).

Spectral simulations to obtain orientation information were performed based on a program developed by Parikh and Allara implemented in MathCad (Mathsoft, Cambridge, MA) in our laboratory. This simulation method utilizes classical electromagnetic wave theory to calculate RAIRS spectra from a series of second-rank optical tensors that describe the layers of the system. We consider four layers: air, phospholipid, alkanethiol, and gold. The optical tensors used for the air and gold layers are isotropic and the optical tensors for the octadecanethiol and DPPC layers were anisotropic, and were determined using the methods described (Parikh and Allara, 1992). The program was used to solve equations describing wave propagation through the layers using a matrix transfer method for a series of model layers, where each set of model layers incorporated a lipid layer with different optical tensors to describe different orientations of the acyl chains. IR absorbance spectra of bulk polycrystalline (solid) samples of octadecylsulfide (Aldrich) and DPPC in the form of KBr pellets were used as reference data.

Impedance measurements were made as described previously (Plant, 1993) in 1 mol/l KCl with a Solartron electrochemical interface (Model 1250, Schlumberger, Hampshire, England) and frequency generator (Model 1286, Schlumberger). The dc potential was held at 0 volts and a sinusoidal ac potential of ± 10 mV was applied at frequencies between 10 and 64,000 Hz. The gold-coated surface that supported the alkanethiol monolayer or phospholipid/alkanethiol HBM was used as the working electrode with a nominal area of 0.32 cm^2 in a three-electrode cell. Data were fit by nonlinear least squares analysis to a simple equivalent circuit consisting of a resistor in series with a capacitor (Plant, 1993). The capacitance of a dielectric layer is related to the thickness, d, of the layer and its dielectric constant, κ, by the following relationship:

$$C_m = \frac{\epsilon_0 \kappa}{d}$$

where C_m is the specific capacitance (normalized by surface area), and ϵ_0 is the permittivity of free space.

For the neutron reflectivity measurements the sample consisted of a single HBM, prepared by transfer of DPPC from the air-water interface as described above, in contact with a D_2O solution. The cell was designed to minimize the incoherent background scattering from the D_2O by minimizing the thickness of the solution. This was achieved by sandwiching a thin Teflon gasket, ~50 μm thick, between the sample and a second silicon block. The neutron beam enters and exits through the silicon block on which the gold film and the HBM sample were deposited, and is reflected from both the HBM surface and from the second silicon substrate on the other side of the aqueous reservoir.

Neutron reflectivity measurements were performed at the BT7 spectrometer at the National Institute of Standards and Technology (Majkrzak, 1991). Filtered, monochromatic (2.35 Å) neutrons are collimated by two slits, defined by absorbing masks, located before the sample position. Neutrons impinge on the sample at a glancing angle, θ, from the plane of the surface. Specularly reflected neutrons are detected by a highly (>90%) efficient ^{3}He detector at an angle of 2θ.

The intensity of the specular reflection is measured as a function of angle of incidence by performing standard θ-2θ scans. The incident beam of wavevector $\mathbf{k}_i$ strikes the first surface at the angle, θ, and the reflected beam of wavevector $\mathbf{k}_f$ exits at the same angle. The reflectivity is measured as a function of the wavevector transfer, $Q = |\mathbf{k}_f - \mathbf{k}_i|$ in the Z direction, normal to the bilayer surface. The intensity of specularly reflected neutrons was measured for wavevector transfers up to $Q \sim 0.25$ Å $^{-1}$, covering up to seven orders of magnitude in reflected intensity. Data were taken at ~160 θ values. Background scattering was determined at every second θ position by measuring the off-specular scattering at an angle of 2θ plus an offset appropriate to θ and the width of the specular peak. The offset varied from 0.1° at $\theta = 0°$ to a maximum of 0.6° at $\theta = 4.0°$. In order to correct for the slit opening size at a given angle, the intensity at $\theta = 2\theta = 0°$ was measured for each slit configuration used in the θ-2θ scan. After subtracting the background intensity from the specular reflectivity data, the data were divided by the slit intensity at each point and then converted to a $\log_{10}$ (reflectivity) versus Q scale.

The HBM can be modeled as a series of three layers, with an average neutron scattering length density (SLD) for each layer. The layers are the sulfur bound to the gold surface, the hydrocarbon chain region, and the phospholipid headgroup region. Both model-independent and model-dependent methods were used to fit the data. In the model-independent method (Berk and Majkrzak, 1995), the SLD profiles are composed of randomly initialized smooth functions represented by parametric B-splines. In general, this method leads to one or more families of solutions that fit the reflectivity data equally well and thus allow a determination of the possible SLD profiles. The SLD profiles can then be quantified using the model-dependent method (Ankner and Majkrzak, 1992), in which the SLD profiles are composed of histogram functions based on the presumed HBM composition. Here, all portions of the lipid which are not explicitly part of the CH_2 chains have been considered collectively as the "lipid headgroup," which includes the carbonyl moieties of the fatty acyl ester bonds. Reflections from the back silicon substrate make a significant contribution to the total reflectivity and were taken into account when analyzing the reflectivity data in both cases.

RESULTS AND DISCUSSION

The amphiphilic character of phospholipids determines their orientation at the surface, which is controlled by the interaction of the polar headgroup region of phospholipids with water, and the affinity between the hydrophobic alkane chains of the two layers. Thus, the configuration of the bilayer that is depicted in Fig. 1 is well founded in the principles of thermodynamics. In addition, a large body of evidence has accumulated in this laboratory that confirms that orientation (Plant, 1993; Plant et al., 1994, 1995; Rao et al., 1997; Meuse et al., 1998).

The data presented here focus on the structure of the bilayer that is formed by the transfer of a phospholipid monolayer from the air-water interface to a support on which an alkanethiol monolayer is assembled. When the samples are initially lifted from the air-water interface, sufficient lipid is removed to result in a transfer ratio of 200%; i.e., two layers of lipid are apparently removed from the interface. The surface also appears wet. After the surface has apparently been dried under a stream of nitrogen, a broad absorbance centering around 3400 cm^{-1} in the RAIR spectra of these samples indicates that there is still water associated with them. RAIRS and ellipsometry data indicate that significantly more lipid is associated with these samples than is seen for a bilayer. Examination with AFM suggests the presence of a readily deformable layer that is perturbed by the AFM tip. When the sample is blotted on filter paper after having been lifted from the air-water interface, the water layer is removed along with the excess lipid molecules. The broad absorbance at 3400 cm^{-1} disappears, and the intensities of the CH_2 and CH_3 bands are smaller and consistent with addition of a single monolayer of lipid. The blotted sample can be scanned repeatedly by AFM without perturbation.

Structure of air-stable HBMs in air

Thickness of the phospholipid layer

Ellipsometry is a convenient method for determining the thickness of the lipid layer of HBMs. A two-layer model was used in which optical constants for the alkanethiol-coated gold layer were determined independently, and were used to determine the thickness of the phospholipid layer of the HBM, assuming a refractive index, n, of 1.45 for the phospholipid. Attempts to use a three-layer model to distinguish between phospholipid acyl chains ($n = 1.45$) and headgroups ($n = 1.33$ to 1.45) were unsuccessful in resolving these portions of the molecule as discrete layers. Our ellipsometry data indicate the thickness of the entire phospholipid layer is 31 ± 1.7 Å.

Continuity of the HBM

AFM was used to assess the continuity of the bilayer structure. While the ellipsometry data suggest the addition of a monolayer of phospholipid to the alkanethiol monolayer, these data reflect an average thickness over a relatively large sample area (hundreds of μm). We used AFM to provide data regarding whether there were patches of phospholipid or if the phospholipid formed a contiguous layer. For this purpose, we performed the AFM measurements in air in the contact mode and examined relatively large areas. Fig. 2 shows representative images collected at a contact force of 60 mN over scanned regions of 1 μm by 1 μm. A gold substrate prepared by thermal deposition and ion milling was compared with a similar substrate that was coated with alkanethiol and phospholipid. These experimental conditions preclude high resolution information, but they provide us with a clear indication that bilayer coverage was apparently complete and homogeneous over large areas. Differences in heights of 3 to 6 nm would be expected if there were patches of alkanethiol monolayer that were not covered with a phospholipid layer, or if the phospholipid layer flipped onto itself to form areas of phospholipid bilayers. No evidence of such inhomogeneity was observed.

Order in the phospholipid alkyl chains

Infrared spectroscopy has long been used to characterize the structure of lipid bilayer preparations and alkanethiol monolayers. Recently we have used surface enhanced Raman spectroscopy and RAIRS to characterize the changes that occur in the alkanethiol monolayer when the phospholipid layer is added. By comparing spectra of samples with and without a phospholipid layer to previous studies of lipids and alkanethiols, we were able to assign the bands we observed for the HBM (Meuse et al., 1998). Fig. 3 (*spectrum a*) shows a RAIRS spectrum of the phospholipid layer of an HBM obtained by making a ratio of the spectrum of an HBM to that of the corresponding alkanethiol. The ratio effectively removes the spectral contributions of the alkanethiol layer and allows us to examine the phospholipid layer. This spectrum clearly shows bands from both the alkane chains and the phosphatidylcholine headgroups. Bands from the headgroups include the band near 1737 cm^{-1} from the ester carbonyl stretching mode, the band near 1100 cm^{-1} from the phosphate symmetric stretching mode, and the band near 1075 cm^{-1} from the ester C—O symmetric stretching mode. Bands from the acyl chains include the band near 1465 cm^{-1} from a CH_2 scissoring mode, the band near 1378 cm^{-1} from the symmetric bending mode of the CH_3 group on the end of the chains, and a series of bands in the 1100 cm^{-1} to 1400 cm^{-1} region where CH_2 wagging progression modes occur.

Previous work (Parikh et al., 1995; Meuse et al., 1998) has found that wagging progressions are too weak to be observed in alkanethiols. When observed in phospholipids,

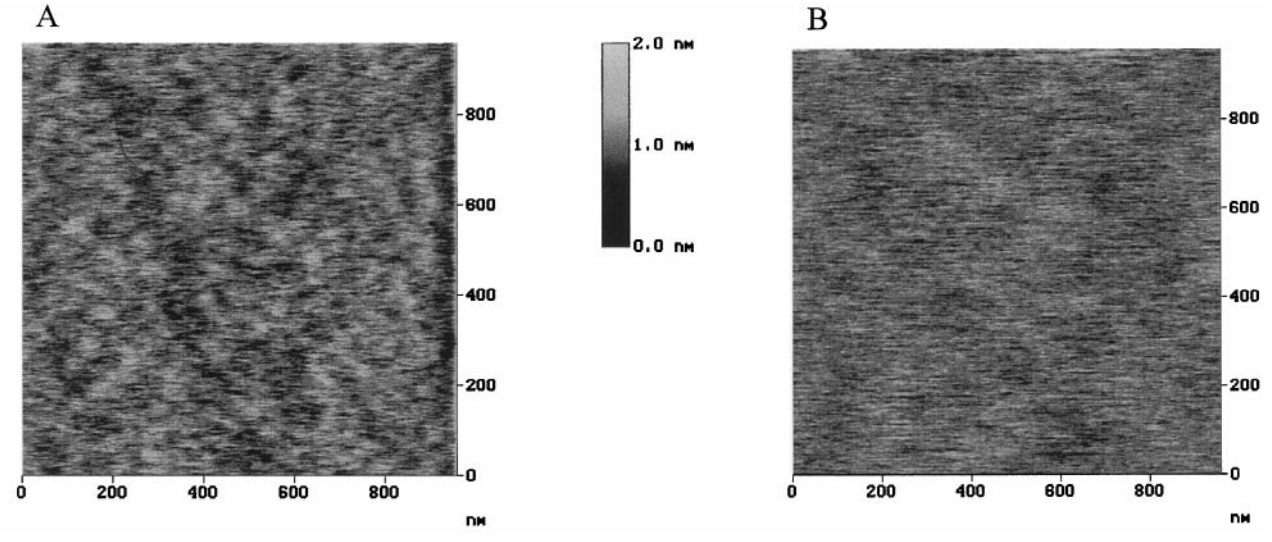

FIGURE 2 (*A*) AFM in air of bare gold substrate; (*B*) AFM in air of HBM surface

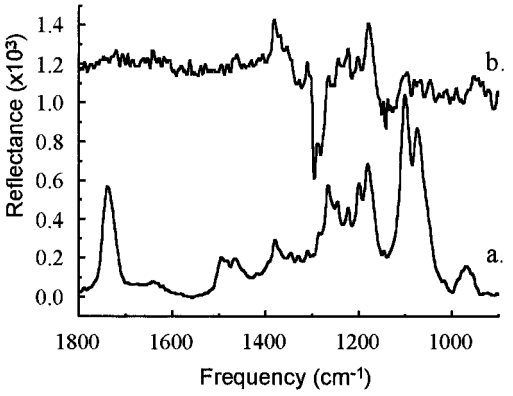

FIGURE 3 (*a*) RAIRS spectrum of a DPPC layer formed by transfer from the air-water interface; (*b*) difference spectrum of hydrogenated DPPC minus deuterated DPPC, leaving only bands associated with the phospholipid acyl chains.

their presence suggests a high degree of intramolecular order (Snyder and Schachtschneider, 1963). To confirm that these features are wagging progressions, HBMs were formed with DPPC in which the hydrogens atoms in the acyl chains were replaced with deuterium atoms. A spectrum of an HBM composed of DPPC-d_{62} was subtracted from the spectrum of an HBM composed of DPPC and the result is shown in Fig. 3 (*spectrum b*). The subtraction eliminates the contributions of the lipid headgroup vibrations but retains C—H vibrations from the acyl chains, since C—D vibrations are spectrally distinct from C—H vibrations. The remaining features are thus due only to the hydrogenated acyl chains of the phospholipid. The wagging progression bands are still clearly present. This treatment confirms the notion that the wagging progressions are from the acyl chains of the phospholipid layer and allows us to more clearly evaluate the separations between the wagging progression bands without interference from the spectral contributions from the phospholipid headgroups.

The separations between these wagging progression bands, $\Delta\nu$, can be related to the number of *trans* bonds contributing to the wag-twist modes, **m**, by Parikh et al. (1995):

$$\Delta\nu = 326/(\mathbf{m} + 1)$$

Table 1 reports a collection of values of **m** for a series of HBMs prepared from phospholipid vesicles or by transfer of phospholipid from the air/water interface, and compares these values to those expected from all *trans* chains.

These values indicate that for several phospholipid chain lengths, and for samples prepared either from vesicles or from by transfer of lipid from the air/water interface, the phospholipid layers of HBMs in air behave similarly and have an average of one *gauche* bond per chain. This would be expected for DPPC and DSPC since, at room temperature, they are well below their gel to liquid crystalline phase transition temperatures of 41°C and 55°C, respectively. The wagging progression bands for DPPC at 15°C, for example, indicate that 98% ± 5% of the bonds are *trans* (Senak et al., 1992). However, the gel-to-liquid crystalline phase transition temperature of DMPC is 23°C, and DMPC might be expected to be more disordered at room temperature. One explanation for the highly ordered structure of DMPC in an HBM in air is that a lower degree of lipid hydration is known to raise the transition temperature (Caffrey et al., 1994). In addition, differential scanning calorimetry has shown that the melting temperature of DPPC associated with silane monolayers covalently bound to glass beads is nearly 9° degrees higher than for DPPC in vesicles (Linseisen et al., 1997).

As indicated above, the infrared spectra of the phospholipid layers of HBMs show a high degree of ordering and conformations similar to those of gel phase lipid bilayers. In order to interpret the spectra with respect to the orientation of the acyl chains of the phospholipids, we have simulated the C—H stretching region of the RAIRS spectra of the DPPC portion of the HBMs using our adaptation of a program developed by Parikh and Allara for the simulation of RAIRS data of alkanethiols (Parikh and Allara, 1992). The best fit simulated spectrum (*dashed line*) is shown in Fig. 4, along with the spectra for the HBMs prepared by transfer from the air-water interface (*dotted line*) as well as for HBMs prepared by from vesicles (*solid line*). The average orientation of the acyl chains is described by tilt (θ), twist (ψ), and azimuth (ϕ) angles as shown in the inset of Fig. 4. The simulation results indicate angles of 34°, −38°, and 50°, respectively, for the acyl chains of DPPC in HBMs.

The comparison of these simulated spectra to the measured spectra indicate several interesting observations. The phospholipid layers can be described as uniaxial with the azimuthal angle having little effect on the simulated spectra.

TABLE 1 Analysis of the wagging progression modes and the number of *trans* bonds in HBM phospholipids in air at room temperature as a function of lipid chain length and method of HBM sample preparation

Lipid/Method	Number of Bonds	Frequency Shift (cm^{-1})	Number of *trans*	% *trans* Bonds
DSPC: air-water interface	17	19.8 ± 0.7	15.5 ± 0.6	91.2 ± 3.5
DPPC: air-water interface	15	21.3 ± 0.9	14.3 ± 0.6	95.3 ± 4.0
DPPC: vesicles	15	21.9 ± 0.9	13.9 ± 0.6	92.6 ± 4.0
DMPC: air-water interface	13	26.5 ± 2.1	11.3 ± 0.9	86.9 ± 6.9
DMPC: vesicles	13	25.4 ± 1.7	11.8 ± 0.8	90.8 ± 6.1

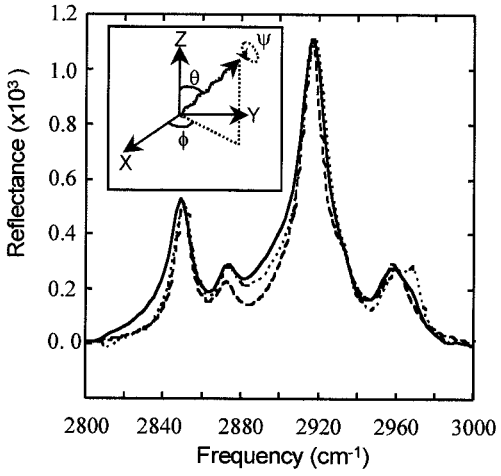

FIGURE 4 RAIRS spectrum of the C—H stretching region of HBMs ratioed to an octadecanethiol monolayer. A DPPC layer added by transfer from the air-water interface (· · ·); a DPPC layer added from phospholipid vesicles in situ (—); a simulated spectrum (- - -). *Inset*: Description of acyl chain orientation angles.

The conformation of the terminal C—C bond of the acyl chains in the HBMs is different from the all *trans* conformation assumed for the polycrystalline reference spectrum from which the optical constants are derived. Achieving maximal correlation between the simulated and the experimental spectra in the intensity of the asymmetric CH_3 band near 2960 cm^{-1} requires the inclusion of one terminal *gauche* bond in a portion of the acyl chains. The exact proportion of terminal *gauche* configurations cannot be determined since the intensity of the asymmetric CH_3 band has previously been found to be insensitive to the number of terminal *gauche* bonds between 10% and 45% for the alkanethiols (Parikh and Allara, 1992).

A comparison of the simulated spectrum to the experimental spectra suggest that angles for the chain tilt, twist, and azimuth are the same regardless of the method of preparation of the HBMs. In addition, we know that there is a similar proportion of *gauche* bonds per chain for the two preparation methods. However, the spectra of the phospholipid layer of the HBMs prepared from the air-water interface and from vesicles are not identical. For example, the samples prepared from the air-water interface (*dotted line* in Fig. 4) have a band at 2964 cm^{-1}. This band could be the result of splitting into in-plane (2964 cm^{-1}) and out-of-plane (2957 cm^{-1}) antisymmetric methyl stretching bands. Splitting of this band has been observed at low temperatures in alkanes and alkanethiols, and suggests a reduction of molecular motion (MacPhail et al., 1982; Nuzzo et al., 1990).

Structure of HBMs in water

The analyses described up to this point provide structural and conformational information about HBMs in air. It is also important to know that HBMs prepared in air can be rehydrated. This was demonstrated with impedance analysis and neutron reflectivity measurements.

Impedance analysis

The magnitude of the impedance of an electrode is determined by the thickness and the dielectric constant of the dielectric layer associated with the electrode surface. The gold substrate supporting an HBM of octadecanethiol and DPPC transferred from the air-water interface served as the working electrode. The impedance magnitude as a function of the frequency of the applied potential (6.4×10^4 Hz to 10 Hz) was fit to an equivalent circuit model consisting of a capacitor (the membrane) in series with a resistor (the electrolyte solution) (Plant, 1993). The specific capacitance was determined to be 0.8 $\mu F\ cm^{-2}$. The electrochemical cell was then rinsed with ethanol in order to remove the DPPC layer while keeping the alkanethiol layer intact. Impedance analysis after rinsing resulted in a capacitance due to the octadecanethiol layer of 1.1 $\mu F\ cm^{-2}$. The capacitance due to the addition of the lipid layer ($C_{\text{m-PL}}$) can be calculated from the value for the capacitance of the alkanethiol monolayer ($C_{\text{m-monolayer}}$) and the capacitance of the phospholipid/alkanethiol bilayer ($C_{\text{m-bilayer}}$) by the following relationship:

$$\frac{1}{C_{\text{m-PL}}} = \frac{1}{C_{\text{m-bilayer}}} - \frac{1}{C_{\text{m-monolayer}}}$$

This analysis leads to a capacitance of 2.9 $\mu F\ cm^{-2}$ for the lipid layer. For comparison, HBMs were formed in situ in the electrochemistry cell by the addition of DPPC vesicles in solution to an octadecanethiol monolayer-coated electrode. In situ measurements allow us to follow the change in capacitance with time, as phospholipid covers the alkanethiol layer, until a limiting capacitance is reached, indicating full coverage of the surface with lipid (Plant, 1993). The capacitance of the octadecanethiol layer was determined to be 1.1 $\mu F\ cm^{-2}$. After several hours in the presence of vesicles equilibrium was achieved, and the capacitance measured was 0.8 $\mu F\ cm^{-2}$. Thus HBMs formed by the transfer of lipid from the air-water interface appear to be identical in dielectric thickness to HBMs formed in situ from phospholipid vesicles.

Neutron reflectivity

While capacitance measurements allow the calculation of the thickness of the dielectric layer in water, there is ambiguity associated with the assumption of an appropriate dielectric constant (Plant et al., 1994). Neutron reflectivity can provide more precise information about the absolute thickness of the layer. Recently, a novel experimental configuration for reflectivity allowed the determination of the structure of a single phosphatidylcholine bilayer adsorbed onto a planar silicon surface in an aqueous environment (Krueger et al., 1995; Koenig et al., 1996). By decreasing

the incoherent background scattering from the water phase, the angular range of neutron reflectivity measurements has been extended and the resolution of the measurements has been increased. The specular reflectivity measurements reported here were sensitive to changes in overall bilayer thickness to within 1–2 Å. A schematic of the cell used for the neutron reflectivity measurements is shown in cross-section in Fig. 5.

In Fig. 6, the reflected intensity from a DPPC/octadecanethiol HBM in D_2O, measured at 60°C, is plotted on a log scale versus Q, the momentum transfer, along with the data from the blank gold substrate. The presence of the HBM has an obvious effect, as the reflected intensity from the HBM is significantly higher than that from the blank at most values of Q. The solid line in the figure represents the best model-dependent fit to the data. The dotted line is an alternative fit to the data.

The difference between the two lines drawn to fit the data in Fig. 6 is shown in Fig. 7, where models of scattering length densities are plotted. The location of each layer in the model is labeled on the graph. The squared profile (*dotted line*) in Fig. 7 is the SLD profile that results if sharp interfaces between layers are assumed. This model corresponds to the dotted line in Fig. 6. The smoother profile in Fig. 7 (*solid line*) corresponds to the solid line fit in Fig. 6, and reflects the profile expected if there is some mixing between layers such that the interfaces between layers are gradual. By comparing these models to the data in Fig. 6, it is clear that the smoother SLD profile (*solid line*) fits the data better. This indicates that the data are better described as interfaces where differences between layers are less discrete than by a model in which sharp differences exist between component layers. It is significant to note that this information about the roughness of the interface is only apparent for scattering data collected above 0.15 $Å^{-1}$. Measurements at lower angles cannot provide this information, since below $Q = 0.18$ the two profiles fit the data equally well. The numerical values for SLD and thickness corresponding to these SLD profiles are listed for each layer in Table 2. The differences in the fitted versus theoretical values in the SiO_2, chromium, and gold layers indicate that there is a significant degree of mixing between these layers.

For analysis of the neutron scattering results, the HBM is modeled as three layers: the sulfur, the hydrocarbon layer

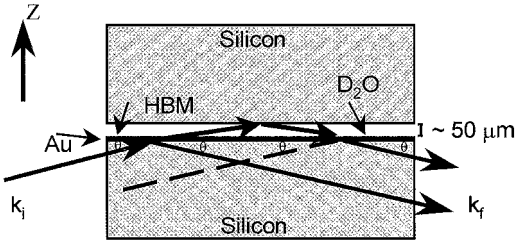

FIGURE 5 Cross-sectional view of the experimental setup used for neutron reflectivity studies. The neutron beam enters and exits through the gold-coated silicon substrate containing the HBM.

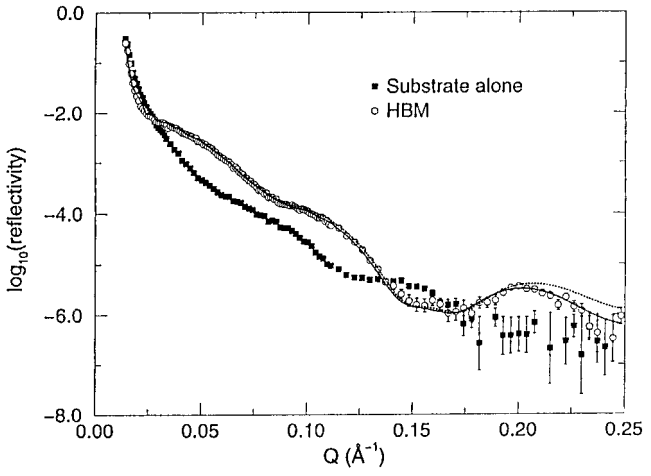

FIGURE 6 Log_{10}(reflectivity) versus Q from a DPPC/octadecanethiol HBM in D_2O, measured at 60°C. The data from the gold-coated silicon substrate alone is shown for comparison. The solid line through the data points represents the best model-dependent fit to the data, and assumes interfaces that are not discrete. The dotted line assumes sharp interfaces (refer to Fig. 7).

corresponding to the alkane chains of both the alkanethiol and the DPPC, and the headgroup layer of the DPPC, which includes the carbonyl groups. The total thickness of the HBM at 60°C is 49 ± 1 Å. The fitted values of the SLDs for the sulfur and CH_2 layers agree with the theoretical values based on the molecular composition, and this indicates that the overall coverage of the surface is close to 100%. If a portion of the substrate was not covered, and thus was exposed to the D_2O solution, the SLD for the sulfur and CH_2 layers would be higher, due to a contribution from the higher SLD of the D_2O. The SLD for the lipid headgroup (LHG) portion of the phospholipid layer is much higher than the theoretical value, indicating that there is a significant amount of hydration in the layer. We do not report a value for the D_2O layer, since sealing the aqueous D_2O

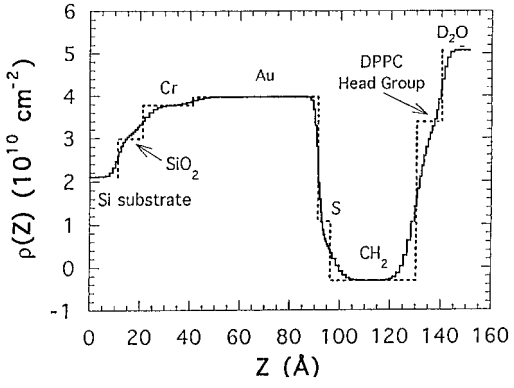

FIGURE 7 Neutron scattering length density profiles from the model-dependent fits of the DPPC/octadecanethiol in D_2O data shown in Fig. 6. The SLD, $\rho(Z)$, is plotted versus Z, the distance perpendicular to the silicon substrate. The dotted profile results if sharp interfaces between the layers are assumed; the solid line is the result of assuming that the interfaces are not discrete.

TABLE 2 Neutron scattering length density (SLD) and thickness of layers in fitted SLD profile for DPPC/octadecanethiol HBM in D_2O, measured at 60°C and 20°C

	Theoretical	Fitted			
Layer	SLD (10^{10} cm^{-2})	SLD (10^{10} cm^{-2}) (60°C)	Thickness (Å) (60°C)	SLD (10^{10} cm^{-2}) (20°C)	Thickness (Å) (20°C)
SiO_2	3.78	3.0 ± 0.2	10 ± 1	3.0 ± 0.2	10 ± 1
Cr	3.03	3.8 ± 0.2	20 ± 1	3.8 ± 0.2	20 ± 1
Au	4.5	4.0 ± 0.2	50 ± 1	4.0 ± 0.2	50 ± 1
S	1.07	1.07 ± 0.05	5.0 ± 0.5	1.07 ± 0.05	5.0 ± 0.5
CH_2	−0.36 (60°C) −0.41 (20°C)	−0.3 ± 0.1	33.0 ± 0.5	−0.3 ± 0.1	35.5 ± 0.5
DPPC LHG	1.79*	3.4 ± 0.2	10 ± 1	3.4 ± 0.2	13 ± 1

*Assuming no hydration.

between the silicon substrates using the thin Teflon gasket resulted in a distortion of the silicon surfaces from perfect flatness. This precluded accurate measurement of the critical angle, which makes determination of the scattering length density of the D_2O problematic.

The hydrocarbon layer of the HBM is composed of alkane associated with the octadecanethiol, and alkane from the acyl chains of DPPC. The contribution to the thickness of the hydrocarbon layer that is due to DPPC is determined by the ratio of the number of carbon atoms in the DPPC alkane chains relative to the number in the thiol alkane chains, and the relative tilts of the chains with respect to the bilayer normal. We assume a tilt of 28° ± 2°and 33° ± 1° for the alkane chains of the thiol (Ulman, 1991) and the DPPC (Tristram-Nagle et al., 1993; and results reported here), respectively.

We examined HBMs composed of DPPC and octadecanethiol at two temperatures, 60°C, which is above the phase transition temperature of DPPC in hydrated bilayers, and 20°C, which is below the phase transition temperature. Fully hydrated DPPC in vesicles undergoes a transition from the more ordered gel phase to the more fluid liquid crystalline phase at a temperature of ~41°C. Since octadecanethiol monolayers are extremely well ordered, and infrared spectroscopy indicate that only a slight decrease in ordering occurs in docosylthiol at 100°C (Nuzzo et al., 1990), we treat all of the temperature-dependent changes we observe as being due to changes in the DPPC. Fig. 8, *top* shows the different specular reflectivity curves for HBMs at 60°C and 20°C, and the best model-dependent fits to the data. The minimum in the 20°C data is located at a slightly lower Q value than that in the 60°C data, indicating that the HBM is slightly thicker in the gel phase than in the liquid crystalline phase. The corresponding SLD profiles for these fits are plotted in Fig. 8, *bottom*. These fitted values for SLD and thickness can also be found in Table 2. The thickness of the hydrocarbon chain region at 20°C, 35.5 ± 0.5 Å, is 1–2 Å larger than the 33.0 ± 0.5 Å measured at 60°C. Assuming that the thickness of the alkane region of the alkanethiol layer remains constant at 19.8 ± 0.7, we determine 15.7 ± 0.5 and 13.2 ± 0.9 Å to be the thickness of the gel and liquid crystalline hydrocarbon chains of DPPC. These data correspond very well to values determined by x-ray diffraction (Nagle and Wiener, 1988; Sun et al., 1994; Nagle et al., 1996; Wiener et al., 1989). Table 2 also indicates an increase of 2–3 Å in the thickness of the LHG layer in the gel phase compared to the liquid crystalline phase DPPC.

The total thickness of the DPPC consists of the thickness of the lipid hydrocarbon layer, $d_{HC,}$ plus the thickness of the lipid headgroup, d_{LHG}. Table 3 shows a comparison of these neutron reflectivity data with x-ray data from the literature. We have calculated the volume of the DPPC hydrocarbon and headgroup regions using our measured thicknesses of

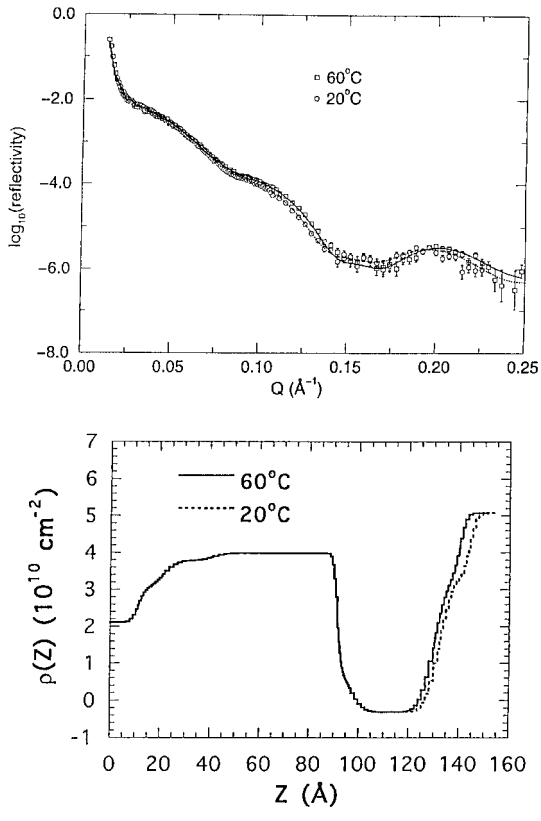

FIGURE 8 *Top:* Log_{10}(reflectivity) versus Q from a DPPC/octadecanethiol HBM in D_2O at 60°C and 20°C. The lines through the data points represent the best model-dependent fits to the data, assuming interfaces that are not discrete. *Bottom:* Resultant SLD profiles from the 60°C data and the 20°C data.

TABLE 3 Comparison of neutron reflectivity data for the DPPC layer of HBMs to x-ray diffraction data for DPPC multilayers

Reference	V_{tot} Dry (Å^3)	V_{HC} (Å^3)	V_{LHG} Dry (Å^3)	d_{tot} (Å)	d_{HC} (Å)	d_{LHG} (Å)	A_{tot} (Å^2)	n_w
Liquid Crystalline Phase								
This work	1229	898	330	23.2 ± 1.3	13.2 ± 0.5	10 ± 1	68.0 ± 4.6	11.7 ± 3.4
Nagle and Wiener, 1988	1232	884	348	20.5–23.4	12.5–15.4	8	64.3–70.9	3.7–7.2
Nagle et al., 1996	1232	884	348	22.6	14.6	8	62.9	6.3
Gel Phase								
This work	1135	792	338	28.7 ± 1.1	15.7 ± 0.5	13 ± 1	50.4 ± 1.6	10.6 ± 2.6
Sun et al., 1994	1148	829	319	25.3	17.3	8	47.9	2.0
Wiener et al., 1989	1144	804	340	26.0	17.5	8.5	45.9	1.7
Nagle and Wiener, 1988	1144	796	348	24.4	16.4	8	48.5	1.3

$d_{tot} = d_{HC} + d_{LHG}$; $V_{tot} = V_{HC} + V_{LHG}$.
n_w = Number of water molecules in LHG region; not equivalent to water between multilayers.

these regions and the partial specific volumes of unhydrated DPPC and DPPC hydrocarbon region (Nagle and Wilkinson, 1978). We determine the volume of the gel phase hydrocarbon region to be 792 Å^3 and the volume of the liquid crystalline phase region as 898 Å^3. The area per lipid molecule calculated from these values is 50.4 ± 1.6 Å^2 for gel-phase DPPC and 60.8 ± 4.6 Å^2 for the liquid crystalline phase. As expected, these values are nearly identical to previously published values based on x-ray data (Nagle and Wiener, 1988; Sun et al., 1994; Nagle et al., 1996; Wiener et al., 1989).

Given this degree of correspondence with x-ray diffraction data, we were surprised to note that our neutron scattering data indicate a thickness for the headgroup region of DPPC which is much larger than that determined from x-ray data. As shown in Table 2, our fitting indicates a scattering length density for the headgroup of 3.4 ± 0.2 × 10^{10} cm^{-2}, and a thickness of 10 ±1 Å and 13 ± 1 Å for the headgroup of liquid crystalline and gel phase DPPC, respectively. These headgroup thicknesses agree well with recent neutron reflectivity data from a single DPPC bilayer on silicon (Koenig et al., 1996).

For both gel and liquid crystalline phase lipid, the SLD which best fit the data was constant, suggesting the same contribution from D_2O in this layer regardless of temperature. Using the partial specific volumes and our determination of headgroup thickness, we can calculate the volume of an unhydrated headgroup of DPPC, and from that infer the hydration of the headgroup region of the DPPC of HBMs. From this calculation, we determine that there are 10.6 ± 2.6 water molecules per lipid in the gel phase, and 11.7 ± 3.4 water molecules per lipid in the liquid crystalline phase, suggesting no significant difference in hydration as a function of the lipid phase. These data are distinctly different from x-ray data on DPPC multilayers. X-ray data have indicated a headgroup thickness on the order of 8 Å (Buldt et al., 1979; Wiener et al., 1989), with only 1 to 2 water molecules associated with the gel phase lipid (Nagle and Wiener, 1988; Sun et al., 1994; Wiener et al., 1989) and 4 to 6 water molecules with the headgroup of the liquid crystalline phase (Nagle and Wiener, 1988; Nagle et al., 1996). These x-ray data suggest a change in thickness of the interlamellar water region but no change in headgroup region thickness with the phase change (Nagle and Wiener, 1988; Sun et al., 1994; Nagle et al., 1996; Wiener et al., 1989). Our data indicate a significantly thicker and more hydrated headgroup region, a large change in headgroup thickness as a function of lipid phase, but only a small (<10%) change in headgroup hydration as a result of the phase change.

The interpretation of our data is not totally unambiguous, since estimates for the extent of hydration and layer thickness are coupled in an inverse relationship. However, attempts to fit the data to different values for the SLD of the headgroup layer resulted in poorer fits. The larger apparent LHG thickness at 20°C could not be compensated for by increasing the SLD without significantly reducing the quality of the fit. The difference that we observe in the neutron reflectivity data in this region between the gel and liquid crystalline phases is on the order of 10%. Regardless of whether this change is due to hydration or thickness, it is very different from the change of approximately a factor of 2 that has been reported for multilamellar systems.

A possible explanation for the discrepancy between these data and the results of x-ray diffraction may lie in the structural differences between the two lipid systems. X-ray data were collected on multilayers of DPPC, and HBMs are single bilayers. The interlamellae water spacing in multilayered systems is small, and varies as a function of lipid phase, increasing from ~17 Å in the gel phase to ~25–32 Å for liquid crystalline phase lipid (Sun et al., 1994). Comparison of the data on these two experimental systems leads to questions concerning the nature of the water in contact with lipid headgroups. Are the headgroups of multilayers in contact with "bulk" water? What is the effect of repulsive interactions between headgroups in the opposing layers on their structure and hydration?

There are other differences between the two techniques that may contribute to the apparent differences in these data. There are contrast differences, since the molecular components scatter neutrons and x-rays differently. In addition, multilayers provide many orders of structure, which result in higher resolution in the Z direction. Neutron reflectivity data corresponding to the headgroup thickness are of relatively low precision, with an uncertainty of ~10%. This may reflect roughness of the hydrated interface, which

x-rays may be less sensitive to considering the large contrast between headgroups and D_2O in neutron scattering. We are currently limited in our ability to delineate the location of water within the headgroup region. Since we cannot completely distinguish between changes in thickness and changes in hydration, the effects that we observe with temperature could perhaps reflect differences in the distribution of water in the headgroup region, while not significantly affecting the total number of water molecules per lipid.

CONCLUSIONS

HBMs can be constructed in air by transfer of phospholipid from the air-water interface. These structures are nearly identical to HBMs formed from lipid vesicles. Our RAIRS measurements indicate that the acyl chains of the lipid layer of an HBM in air formed by both methods have approximately one *gauche* bond per chain, and are tilted ~34° from the *z* axis. Impedance spectroscopy shows that the HBMs prepared in air can be reintroduced to an aqueous solution and that they demonstrate the same capacitance measured for HBMs formed in situ from vesicles. This suggests that the HBMs prepared in air are equivalent in dielectric constant and thickness and cover the entire surface. AFM also indicates a continuous layer. Ellipsometry shows that in air, the lipid layer of a DPPC/octadecanethiol HBM is 31.0 ± 1.7 Å thick at room temperature. In water, neutron reflectivity reveals that the lipid layer of an HBM in contact with an aqueous solution has a thickness in the gel state of 28.7 ± 1.1 Å, which is very similar to that observed in air by ellipsometry. The combination of ellipsometric thickness data and RAIRS data on chain tilt, together with AFM and impedance data indicating full surface coverage by the bilayer, allows us to arrive at an unambiguous interpretation of the neutron reflectivity data.

In the previous work with phospholipid bilayers at a silicon surface using a similar experimental setup (Koenig et al., 1996), surface coverage of lipids was estimated to be ~70% to 95%, depending on the sample. One distinct advantage associated with phospholipid/alkanethiol HBMs compared to phospholipid/phospholipid bilayers is the ease of achieving 100% surface coverage of the lipid bilayer.

Success in these reflectivity measurements requires a smooth and thin gold layer on top of the silicon substrate. The thickness of the gold film determines its reflectivity as a function of incident angle; we found that a 50-Å-thick gold film gives a small enough contribution to the overall reflectivity compared to that of the lipid layer to permit sensitive modeling of the layer of interest. Quantifying the structural parameters of the bilayer requires that the gold film must be sufficiently smooth. These conditions were achieved by using an ion-beam/ion-milling technique to fabricate a 50-Å-thick gold film with an RMS roughness of <2 Å as determined by AFM analysis.

While AFM provides information about topographical roughness, neutron reflectivity data provide important information about the compositional roughness of these surfaces. It is clear from the data that there is mixing of silicon and chromium, and chromium and gold. It is clear that the gold-sulfur interface is not sharp either. This may reflect topographical roughness in the gold surface, or subtle alterations in the scattering length density of the components as a result of their chemical interaction, or a combination of these factors. Of greatest interest from the biophysics point of view is the information that this experimental approach may be able to provide about the "roughness" of the phospholipid headgroup area. These measurements of a single bilayer provide a somewhat different picture of the headgroup region than has been reported for multilammellar bilayers, and suggest greater hydration of single bilayer headgroups. With improved spatial resolution, we could perhaps probe more precisely the location of water in the headgroup area of single bilayers. We report here a sensitivity in total layer thickness on the order of 1–2 Å, but currently better spatial resolution can be achieved on multilayered preparations.

To obtain better sensitivity to changes in SLD within a layer, higher resolution measurements are necessary. One straightforward way to achieve this is to measure the reflected intensity out to even higher angles, which generally also means to lower intensities. In practice, such measurements are limited by background scattering from various sources, most notably the incident medium and the aqueous solution. Based on measurements of SiO_2 on silicon in vacuum, it is reasonable to predict that recent instrumental improvements make it possible to measure our sample down to 10^{-8} in reflected intensity (Dura, J. A., C. Richter, and C. F. Majkrzak, manuscript in preparation). Work is currently underway to design a better sample environment so that full advantage can be taken of this new capability. This opens up the possibility of higher resolution measurements of the structure of this model membrane system.

The authors thank Dr. Frank Grunfeld (NIMA Technologies) for helpful discussions regarding the air-water interface.

REFERENCES

Ankner, J. F., and C. F. Majkrzak. 1992. Subsurface Profile Refinement for Neutron Specular Reflectivity. In S.P.I.E. Conference Proceedings, Vol. 1738. C. F. Majkrzak and J. L. Wood, editors. S.P.I.E., Bellingham, WA.

Batzri, S., and E. D. Korn. 1973. Single bilayer liposomes prepared without sonication. *Biochim. Biophys. Acta.* 901:157.

Berk, N. F., and C. F. Majkrzak. 1995. Using parametric B-splines to fit specular reflectivities. *Phys. Rev. B.*, 51:11296–11309.

Buldt, G. H., J. Gally, J. Seelig, and G. Zaccai. 1979. Neutron diffraction studies on phosphatidylcholine model membranes I: headgroup conformation. *J. Mol. Biol.* 134:673–691.

Caffrey, M., J. L. Hogan, R. D. Koynova, and D. Moynihan. 1994. Lipid Thermotropic Phase Transition Database (LIPIDAT2), version 2.0, National Institute of Standards and Technology, Gaithersburg, MD.

Duschl, C., M. Liley, H. Lang, A. Ghandi, S. M. Zakeeruddin, H. Stahlberg, J. Dubochet, A. Nemetz, W. Knoll, and H. Vogel. 1996. Sulphur-bearing lipids for the covalent attachment of supported lipid bilayers to gold surfaces: a detailed characterisation and analysis. *Mater. Sci. Eng.* C4:7–18.

Erdelen, C., L. Haussling, R. Naumann, H. Ringsdorf, H. Wolf, J. Yang, M. Liley, J. Spinke, and W. Knoll. 1994. Self-assembled disulfide-functionalized amphiphilic copolymers on gold. *Langmuir*. 10: 1246–1250.

Florin, E.-L., and H. E. Gaub. 1993. Painted supported lipid membranes. *Biophys. J.* 64:375–383.

Gizeli, E., C. R. Lowe, M. Liley, and H. Vogel. 1996. Detection of supported lipid layers with the acoustic Love waveguide device: application to biosensors. *Sens. Actuators.* B34:295–300.

Johnson, S. J., T. M. Bayerl, D. C. McDermott, G. W. Adam, A. R. Rennie, R. K. Thomas, and E. Sackmann. 1991. Structure of an adsorbed dimyristoylphosphatidylcholine bilayer measured with specular reflection of neutrons. *Biophys. J.* 59:289–294.

Kalb, E., S. Frey, and L. K. Tamm. 1992. Formation of supported planar bilayers by fusion of vesicles to supported phospholipid monolayers. *Biochim. Biophys. Acta.* 1103:307–316.

Koenig, B. W., S. Krueger, W. J. Orts, C. F. Majkrzak, N. F. Berk, J. V. Silverton, and K. Gawrisch. 1996. Neutron reflectivity and atomic force microscopy studies of a lipid bilayer in water adsorbed to the surface of a silicon single crystal. *Langmuir.* 12:1343–1350.

Krueger, S., J. F. Ankner, S. K. Satija, C. F. Majkrzak, D. Gurley, and M. Colombini. 1995. Extending the angular range of neutron reflectivity measurements from planar lipid bilayers: application to a model biological membrane. *Langmuir.* 11:3218–3222.

Lang, H., C. Duschl, M. Gratzel, and H. Vogel. 1992. Self-assembly of thiolipid molecular layers on gold surfaces: optical and electrochemical characterization. *Thin Solid Films.* 210/211:818–821.

Linseisen, F. M., M. Hetzer, T. Brumm, and T. M. Bayerl. 1997. Differences in the physical properties of lipid monolayers and bilayers on a spherical solid support. *Biophys. J.* 72:1659–1667.

Loesche, M., M. Piepenstock, A. Diederich, K. Gruenewald, and D. Vaknin. 1993. Influence of surface chemistry on the structural organization of monomolecular protein layers adsorbed to functionalized aqueous interfaces. *Biophys. J.* 65:2160–2177.

MacPhail, R. A, Snyder, R. G., Strauss, H. L. 1982. The motional collapse of the methyl C—H stretching vibrational bands. *J. Chem. Phys.* 77(3): 1118–1137.

Majkrzak, C. F. 1991. Polarized neutron reflectometry. *Physica B.* 173: 75–88.

Majkrzak, C. F., and G. P. Felcher. 1990. Neutron scattering studies of surfaces and interfaces. *Mater. Res. Soc. Bull.* 15:65–72.

Meuse, C. W., G. Niaura, M. Lewis, A. L. Plant. 1998. Assessing the molecular structure of supported hybrid bilayer membranes with vibrational spectroscopies. *Langmuir*. 14:(in press).

Nagle, J. F., and M. C. Wiener. 1988. Structure of fully hydrated bilayer dispersions. *Biochim. Biophys. Acta.* 942:1–10.

Nagle, J. F., and D. A. Wilkinson. 1978. Lecithin bilayers: density measurements and molecular interactions. *Biophys. J.* 23:159–175.

Nagle, J. F., R. Zhang, S. Tristram-Nagle, W.-J. Sun, H. I. Petrache, and R. M. Suter. 1996. X-ray structure determination of fully hydrated L(alpha) phase dipalmitoylphosphatidylcholine bilayers. *Biophys. J.* 70: 1419–1431.

Naumann, C., C. Dietrich, J. R. Lu, R. K. Thomas, A. R. Rennie, J. Penfold, and T. M. Bayerl. 1994. Structure of mixed monolayers of dipalmitoylglycerophosphocholine and polyethylene glycol monododecyl ether at the air/water interface determined by neutron reflection and film balance techniques. *Langmuir.* 10:1919–1925.

Nuzzo, R. G., E. M. Korenic, and L. H. Dubois. 1990. Studies of the temperature-dependent phase behavior of long chain n-alkyl thiol monolayers on gold. *J. Chem. Phys.* 93:767.

Parikh, A. N., and D. L. Allara. 1992. Quantitative determination of molecular structure in multilayered thin films of biaxial and lower symmetry from photon spectroscopies. I. Reflection infrared vibrational spectroscopy. *J. Chem. Phys.* 96:927–945.

Parikh, A. H., B. Liedberg, S. V. Atre, M. Ho, and D. L. Allara. 1995. Correlation of molecular organization and substrate wettability in the self-assembly of *n*-alkylsiloxane monolayers *J. Phys. Chem.* 99: 9996–10008.

Pedulla, J., and R. D. Deslattes. 1993. Multilayer and Grazing Incidence X-Ray/EUV Optics. R. B. Hoover and A. B. C. Walker, editors. Proc. SPIE 2011, 299.

Plant, A. L. 1993. Self-assembled phospholipid/alkanethiol biomimetic bilayers on gold. *Langmuir.* 9:2764–2767.

Plant, A. L., M. Brigham-Burke, and D. O'Shannessy. 1995. Phospholipid/alkanethiol bilayers for cell surface receptor studies by surface plasmon resonance. *Anal. Biochem.* 226:342–348.

Plant, A. L., M. Guegeutchkeri, and W. Yap. 1994. Supported phospholipid/alkanethiol biomimetic membranes: insulating properties. *Biophys. J.* 67:1126–1133.

Rao, N. M., A. L. Plant, V. Silin, S. Wight, and S. W. Hui. 1997. Characterization of biomimetic surfaces formed from cell membranes. *Biophys. J.* 73:3066–3077.

Reinl, H., T. Brumm, and T. M. Bayerl. 1992. Changes of the physical properties of the liquid-ordered phase with temperature in binary mixtures of DPPC with cholesterol. *Biophys. J.* 61:1025–1035.

Schmidt, A., J. Spinke, T. M. Bayerl, and W. Knoll. 1992. Streptavidin binding to biotinylated lipid layers on solid supports. *Biophys. J.* 63: 1185–1192.

Senak, L., D. Moore, and R. Mendelson. 1992. CH2 wagging progressions as IR probes of slightly disordered phospholipid acyl chain states. *J. Phys. Chem.* 96:2749–2754.

Snyder, R. G., and J. H. Schachtschneider. 1963. Spectrochim. *Acta, Part A.* 19:85.

Stelzle, M., G. Weissmuller, and E. Sackmann. 1993. On the application of supported bilayers as receptive layers for biosensors with electrical detection *J. Phys. Chem.* 97:2974–2981.

Sun, W.-J., R. M. Suter, M. A. Knewtson, C. R. Worthington, S. Tristram-Nagle, R. Zhang, and J. F. Nagle. 1994. Order and disorder in fully hydrated unoriented bilayers of gel phase dipalmitoylphosphatidylcholine. *Phys. Rev. E.* 49:4665–4676.

Tamm, L. K., and H. M. McConnell. 1985. Supported phospholipid bilayers. *Biophys. J.* 47:105–113.

Tien, H. T. 1990. Self-assembled lipid bilayers for biosensors and molecular electronic devices. *Adv. Mat.* 2:316–318.

Tristram-Nagle, S., R. Zhang, R. M. Suter, C. R. Worthington, W.-J. Sun, and J. F. Nagle. 1993. Measurement of chain tilt angle in fully hydrated bilayers of gel phase lecithins. *Biophys. J.* 64:1097–1109.

Ulman, A. 1991. Introduction to Thin Organic Films: From Langmuir-Blodgett to Self-Assembly. Academic Press, Boston.

Vaknin, D., J. Als-Nielsen, M. Piepenstock, and M. Loesche. 1991. Recognition processes at a functionalized lipid surface observed with molecular resolution. *Biophys. J.* 60:1545–1552.

Wiener, M. C., R. M. Suter, and J. F. Nagle. 1989. Structure of fully hydrated gel phase of dipalmitoylphosphatidylcholine. *Biophys. J.* 55: 315–325.